MESSENGER observations of Mercury's magnetosphere during northward IMF

James A. Slavin,[1] Brian J. Anderson,[2] Thomas H. Zurbuchen,[3] Daniel N. Baker,[4] Stamatios M. Krimigis,[2,5] Mario H. Acuña,[6] Mehdi Benna,[6] Scott A. Boardsen,[1] George Gloeckler,[3,7] Robert E. Gold,[2] George C. Ho,[2] Haje Korth,[2] Ralph L. McNutt Jr.,[2] Jim M. Raines,[3] Menelaos Sarantos,[1] David Schriver,[8] Sean C. Solomon,[9] and Pavel Trávníček[10]

Received 28 September 2008; revised 11 November 2008; accepted 18 November 2008; published 17 January 2009.

[1] MESSENGER's January 14, 2008, flyby of Mercury has provided new observations of the planet's magnetosphere for northward interplanetary magnetic field (IMF). The dusk magnetopause was located inward from the mean magnetopause surface, possibly due to reduced tail magnetic flux content for IMF $B_z > 0$ and/or the pressure of planetary pickup ions as they respond to the dawnward $-\mathbf{v} \times \mathbf{B}$ electric field in the magnetosheath. Within the plasma sheet rotations of the magnetic field are observed consistent with, Kelvin–Helmholtz vortices $\sim$1 R_M in diameter (R_M is Mercury's radius). MESSENGER exited through a 1,000 km-wide boundary layer bordered by inner and outer current sheets that resemble rotational and tangential discontinuities, respectively. The total magnetic field change across this layer is consistent with the predicted solar wind ram pressure at Mercury during the MESSENGER flyby. **Citation:** Slavin, J. A., et al. (2009), MESSENGER observations of Mercury's magnetosphere during northward IMF, *Geophys. Res. Lett.*, *36*, L02101, doi:10.1029/2008GL036158.

1. Introduction

[2] The first Mercury flyby by the MErcury Surface, Space ENvironment, GEochemistry, and Ranging (MESSENGER) spacecraft showed that Mercury has a predominantly dipolar magnetic field whose magnitude has changed little or not at all since the Mariner 10 encounters in 1974–1975 [*Anderson et al.*, 2008]. MESSENGER's Fast Imaging Plasma Spectrometer (FIPS) observations revealed that this planet's small magnetosphere is immersed in a cloud of planetary ions that extends beyond the dayside bow shock (BS) [*Zurbuchen et al.*, 2008a; *Slavin et al.*, 2008]. The interplanetary magnetic field (IMF) during the first MESSENGER flyby varied from moderately to strongly northward and has provided our first observations of the low-latitude magnetosphere under such conditions. Here we present the first model of BS and magnetopause (MP) position, boundary wave properties, and boundary current sheet structure for northward IMF from MESSENGER measurements.

2. Mercury Bow Shock and Magnetopause Locations

[3] The trajectories of Mariner 10 and MESSENGER during their flybys of Mercury are depicted in solar wind-aberrated Mercury Solar Orbital (MSO) coordinates in Figure 1a. In the MSO coordinate system, X_{MSO} is directed from the center of the planet toward the Sun, Z_{MSO} is normal to Mercury's orbital plane and positive toward the north celestial pole, and Y_{MSO} completes the right-handed system. The trajectories for the final two MESSENGER flybys on October 6, 2008 and September 29, 2009, are based on current predictions.

[4] The locations of the mean inbound and outbound BS and MP crossings from the MESSENGER and Mariner 10 flybys [*Slavin and Holzer*, 1979; *Slavin et al.*, 2008] are displayed in Figure 1b. An aberration correction of 4° is assumed for the Mariner 10 encounters due to their high solar wind speeds [*Slavin and Holzer*, 1979]. A 7° aberration is applied to the MESSENGER boundary crossings based on average solar wind speed predicted for the time of the flyby by solar – heliospheric models [*Baker et al.*, 2008; *Zieger et al.*, 2008].

[5] The BS crossings have been fit, following *Slavin and Holzer* [1981], using a conic section whose focus is free to lie along the aberrated X axis at $X' = X_o$ where

$$\sqrt{(X' - X_0)^2 + Y'^2 + Z'^2} = \frac{L}{1 + \varepsilon \cdot \cos(\theta)} \quad (1)$$

[1]Heliophysics Science Division, NASA Goddard Space Flight Center, Greenbelt, Maryland, USA.
[2]Johns Hopkins University Applied Physics Laboratory, Laurel, Maryland, USA.
[3]Department of Atmospheric, Oceanic and Space Sciences, University of Michigan, Ann Arbor, Michigan, USA.
[4]Laboratory for Atmospheric and Space Physics, University of Colorado, Boulder, Colorado, USA.
[5]Office of Space Research and Technology, Academy of Athens, Athens, Greece.
[6]Solar System Exploration Division, NASA Goddard Space Flight Center, Greenbelt, Maryland, USA.
[7]Department of Astronomy, University of Maryland, College Park, Maryland, USA.
[8]Institute for Geophysics and Planetary Physics, University of California, Los Angeles, California, USA.
[9]Department of Terrestrial Magnetism, Carnegie Institution of Washington, Washington, D.C., USA.
[10]Astronomical Institute, Academy of Sciences Czech Republic, Prague, Czech Republic.

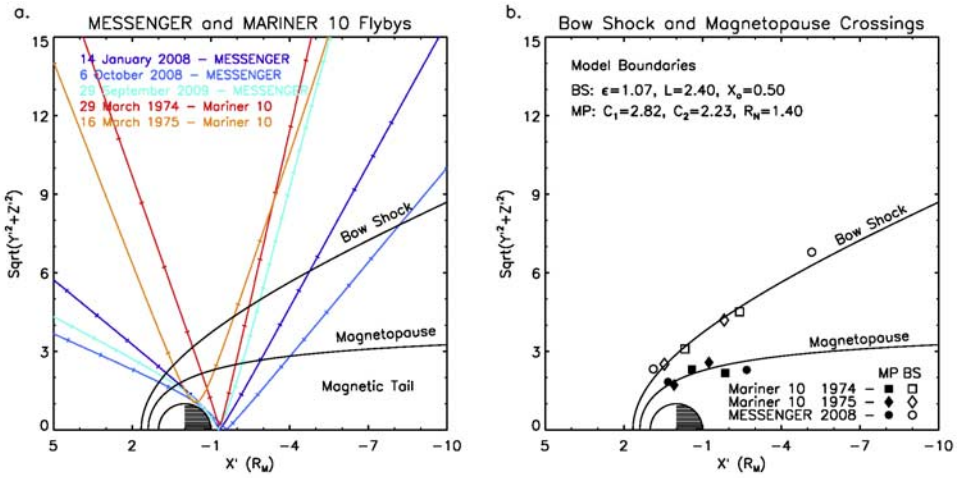

Figure 1. (a) Mariner 10 and MESSENGER Mercury flyby trajectories are displayed in solar-wind-aberrated cylindrical MSO coordinates. (b) Averaged inbound and outbound bow shock (BS) and magnetopause (MP) crossings are shown for the three flybys that have taken place to date. Model boundaries based on the flyby observations are displayed along with best-fit parameters.

and the eccentricity, ε, and the semi-latus rectum, L, are the other two parameters determined from linear least-square fitting. The polar angle θ is measured from the $+X'$ axis about X_o to the radial vector from the focus to the crossing. As shown in Figure 1b, an excellent fit is obtained with X_o = 0.50 R_M, ε = 1.07, and L = 2.40 R_M (R_M is Mercury's radius) with an estimated uncertainty of 5%. The extrapolated nose distance for this model BS is 1.66 R_M. The eccentricity is significantly greater than that seen for the other terrestrial planets [*Slavin et al.*, 1984]. The reason is almost certainly the decrease in solar wind fast mode Mach number with decreasing distance from the Sun. The asymptotic Mach cone calculated from our BS surface corresponds to a solar wind fast mode Mach number of ~3.

[6] The MP crossings have been modeled using the *Howe and Binsack* [1972] formalism, where

$$\sqrt{Y'^2 + Z'^2} = c_1 \tan^{-1}\left(\sqrt{\frac{R_N - X'}{c_2}}\right) \quad (2)$$

The best-fit parameters R_N, c_1, and c_2 were found to have values of 1.40 R_M, 2.82 R_M, and 2.32 R_M, respectively, with estimated uncertainties of 0.1 R_M. The derived solar wind stand-off distance, R_N = 1.4 R_M, is in good agreement with previous results [*Russell*, 1977; *Slavin and Holzer*, 1979]. MESSENGER cannot observe the solar wind, but solar magnetograph-driven models of the solar wind have been used to predict a ram pressure, P_{sw}, of ~16 nPa for the January 14, 2008 encounter [*Baker et al.*, 2008], a value which is near the expected mean. This estimate of P_{sw} and R_N may be used to compute the moment of Mercury from the pressure balance condition for a dipolar magnetosphere:

$$M_o = \left(2\pi k P_{sw} R_N^6 / f^2\right)^{1/2} \quad (3)$$

where k = 0.88 and f = 1.22 describe the drag on the magnetosphere and the effect of the shape of the MP on the magnetic field intensity [see *Slavin and Holzer*, 1979]. The result is $M_o \sim 212$ nT–R_M^3, which is similar to values inferred directly from the MESSENGER and Mariner 10 magnetometer data [*Anderson et al.*, 2008].

3. MESSENGER Magnetic Field Measurements

[7] The MESSENGER trajectory and magnetic field vectors (10-s averages) projected onto the X_{MSO} – Y_{MSO} and Y_{MSO} – Z_{MSO} planes are shown in Figure 2 along with average BS and MP surfaces. An aberration of 7° due to Mercury's orbital motion through the radial solar wind is assumed. The inbound BS (not shown) was crossed at 18:08:38 UTC [*Slavin et al.*, 2008]. Magnetic field observations taken in the solar wind are shown in gold, and the magnetosheath data are in blue. Before the inbound MP crossing at 18:42:57, the IMF had been northward for ~4 min. Following the exit from the magnetosphere at 19:14:15, the IMF in the magnetosheath was observed to be more strongly northward.

[8] The inbound MP crossing occurred closer to the Sun-Mercury axis than predicted by the mean MP model, as shown in Figure 2a. The dusk MP crossing for the first Mariner 10 flyby in Figure 1b also took place under northward IMF conditions and was displaced inward by a similar distance. More observations are needed, but these crossings suggest a systematic inward displacement of the dusk MP for northward IMF. As shown in Figure 2, the inbound MESSENGER MP crossing was characterized by a fast transition to a much quieter magnetic field directed predominantly northward, but with a small sunward component. These magnetic field variations indicate that the spacecraft entered through the dusk flank of the tail into the central plasma sheet (red arrows) just north of the mid-plane of the cross-tail current sheet [*Slavin et al.*, 2008]. As the spacecraft neared the planet the magnetic field intensity began to increase quickly as MESSENGER moved into the

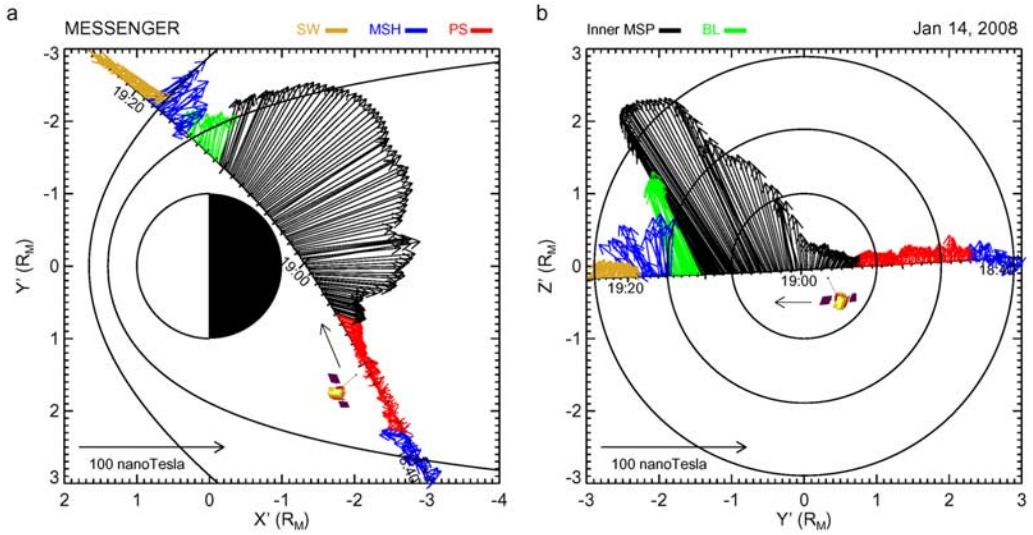

Figure 2. (a) MESSENGER magnetic field vectors (10-s averages) are projected onto the aberrated $X_{MSO}-Y_{MSO}$ plane. (b) Similar display, but for the aberrated $Z_{MSO}-Y_{MSO}$ plane. As indicated, different colors are used to identify the different boundaries and regions of the magnetosphere (SW, solar wind; MSH, magnetosheath; PS, plasma sheet; MSP, magnetosphere; BL, boundary layer). Bow shock and magnetopause model surfaces are also shown.

region dominated by Mercury's dipolar planetary magnetic field [*Anderson et al.*, 2008]. The magnetic field measurements in this region are shown in black in Figures 2a and 2b. The significant tailward tilting of these magnetic fields even close to the planet is due to the presence of a strong cross-tail current sheet. A strong magnetic field decrease, beginning at 19:10:35, corresponds to a current layer perpendicular to the magnetic field as evident by the minimal rotation in direction. Shown in green in Figures 2a and 2b, this interval ended with the MP crossing near the dawn terminator at 19:14:15. As shown, the magnetic field in this region has largely the same orientation as the inner magnetosphere, but it is ~20 nT weaker.

4. Magnetic Field Rotations in the Dusk Plasma Sheet

[9] MESSENGER entered the magnetosphere through the dusk flank of the plasma sheet near the center of the cross-tail current layer [*Slavin et al.*, 2008]. The MP crossing is indicated in Figure 3a by a vertical dashed line. In the adjacent magnetosheath B_x is relatively large and

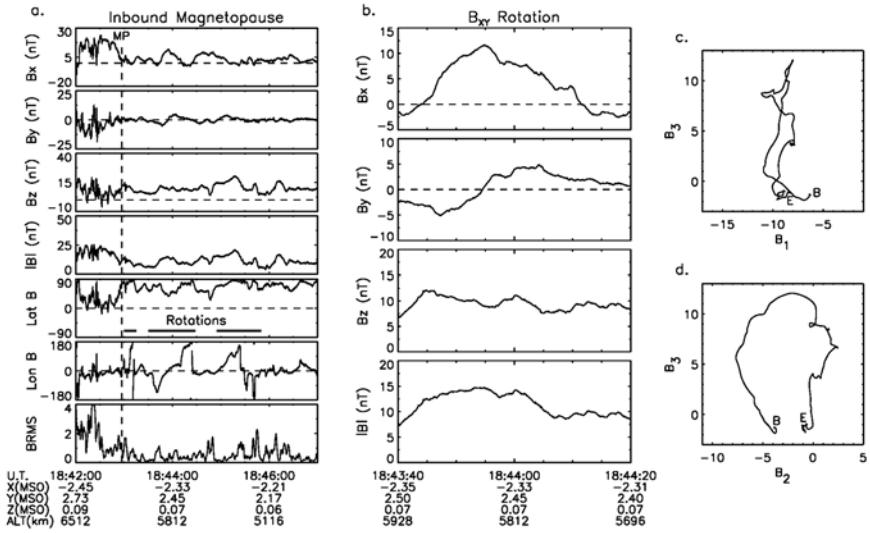

Figure 3. (a) High-time-resolution magnetic field measurements across the inbound magnetopause boundary are displayed in MSO coordinates. Note the intervals where there were large rotations of the magnetic field. (b) Close-up view of one of the rotations. Graphs of the rotation event in the (c) B_3-B_1 and (d) B_3-B_2 planes.

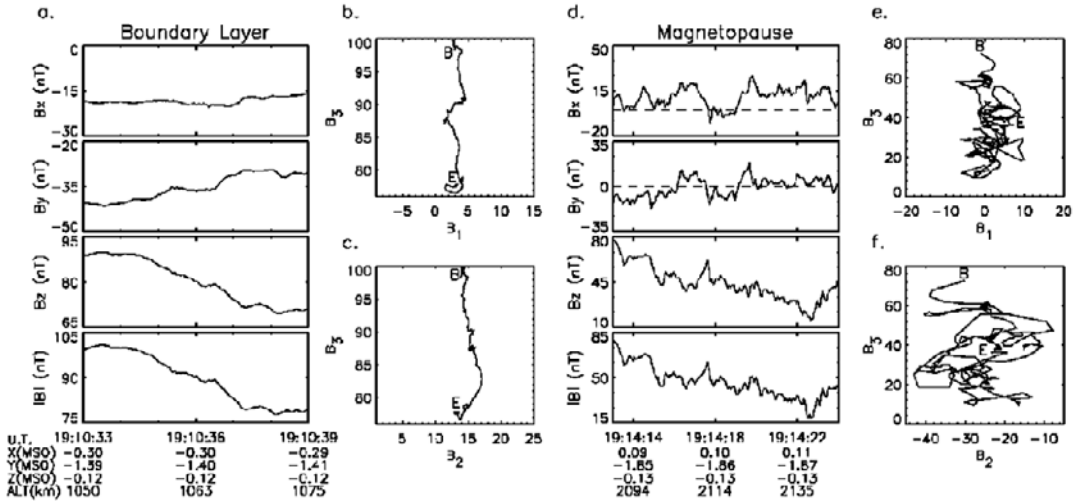

Figure 4. High-time-resolution magnetic field measurements across (a) the inner current sheet and (d) the outbound magnetopause. Graphs of the magnetic field variations across these current sheets in the (b and e) $B_3-B_1$and (c and f) B_3-B_2 planes.

positive while B_y is small, consistent with the draping of a "toward" IMF sector about the magnetosphere. The B_z component is northward with values of ~5 to 10 nT. In the plasma sheet, between 18:43 and 18:46, the magnetic field makes several nearly complete rotations in longitude angle with periods of ~5 to 25 s. Figure 3b shows a close-up of the second rotation observed after the MP crossing. Figures 3c and 3d display hodograms of this rotation in the planes of maximum—minimum and maximum—intermediate variance. The directions of minimum, intermediate, and maximum variance, B_1, B_2, and B_3, in MSO coordinates are (−0.07, 0.22, 0.97), (−0.06, 0.97, −0.22), and (1.0, 0.06, 0.07), respectively. The principal axis directions are well defined, with ratios of intermediate to minimum and maximum to intermediate eigenvalue of 9.4 and 2.5. The hodograms show a relatively smooth rotation of the magnetic field in the B_2-B_3 plane and a steady B_1 magnetic field, which is approximately normal to the plane of the cross-tail current sheet.

5. Boundary Layer and Magnetopause Structure

[10] At 19:10:35, about 1,000 km before MESSENGER crossed the outbound MP, the magnetic field suddenly decreased from ~100 to 80 nT in just ~4 s. The magnetic field in this region is orientated very close to that of the inner magnetosphere as shown in Figure 2 (i.e., green vectors). It has been suggested [*Anderson et al.*, 2008; *Slavin et al.*, 2008] that this region of decreased magnetic field intensity might be considered a "boundary layer" (BL). The inner current sheet across which the magnetic field decreases at the start of the BL is shown in Figure 4a. For comparison the magnetic field measurements across the MP that produced a further decrease from ~65 to 30 nT are shown in Figure 4d. Figures 4b, 4c, 4e, and 4f show hodograms of the magnetic field change across these two current sheets in the planes of maximum—minimum and maximum—intermediate variance.

[11] The magnetic variations across these two thin current sheets have many features in common. If pressure balance is assumed across these current sheets by gradients in plasma pressure, then comparable outward increases in the plasma pressure of ~1.4 and 1.3 nPa, respectively, are required. The orientations of the current sheets are similar, with minimum variance directions in MSO coordinates of (−0.33, −0.82, −0.47) and (0.57, −0.80, −0.18), respectively. If the Newtonian approximation is assumed for the normal pressure, P_n, exerted by the solar wind ram pressure on the MP, i.e., $P_n \sim \sin^2\psi$, where ψ is the angle of incidence of the solar wind flow, then the measured magnetic field change across the MP current sheet implies an upstream pressure of only ~4.2 nPa. However, when the total magnetic field compression across both current sheets is considered a value of ~12 nPa is found, in reasonable agreement with the *Baker et al.* [2008] prediction of ~16 nPa.

[12] The magnetic field component normal to these current sheets (i.e., B_1) is, however, very different. The inner current sheet at the start of the boundary layer resembles a rotational discontinuity with a significant mean normal field component of ~3 nT. The MP current sheet hodograms are much noisier, with large-amplitude fluctuations due to the close proximity of the magnetosheath. However, the normal field component is, on average, small and consistent with the tangential discontinuity structure expected for an MP not undergoing reconnection during northward IMF.

6. Discussion

[13] New models of the BS and MP using all Mariner 10 and MESSENGER crossings show that the BS is more flared than at the Earth and indicates an average fast-mode Mach number of ~3, in good agreement with estimates of the mean values at Mercury orbit. The shape of the MP is similar to that of the Earth, with a nose distance of 1.4 R_M. The stand-off distance of the mean MP is consistent with the average solar wind dynamic pressure and the present values of Mercury's dipole moment. An inward displacement of the dusk flank of the MP from the mean surface was

observed during northward IMF both by MESSENGER and Mariner 10. More measurements are needed, but these displacements may be due to a reduction in tail magnetic flux content associated with IMF $B_z > 0$ and/or the pressure exerted by newly created planetary pickup ions reacting to the dawnward $-v \times \mathbf{B}$ electric field in the magnetosheath for northward IMF. Indeed, the MESSENGER inbound MP crossing coincided with the most intense fluxes of planetary ions measured except for closest approach [*Zurbuchen et al.*, 2008a]. Further evidence for a strong asymmetry in planetary pickup ion acceleration and penetration into the dusk flank of the magnetosphere for IMF $B_z > 0$ is found in the single particle Na^+ tracings of *Sarantos et al.* [2008].

[14] MESSENGER's first flyby also produced strong evidence for Kelvin Helmholtz (K-H) vortices [*Slavin et al.*, 2008]. Rotational signatures in the plasma sheet magnetic field observed near the dusk flank of the tail are similar to those at the flanks of the Earth's tail that have been modeled as K-H vortices by *Otto and Fairfield* [2000]. Their simulations successfully reproduced the $\sim$1–5-R_E spatial scales and 5–10-min periods of the vortices observed in the terrestrial magnetic field and plasma velocity data. For Earth-like anti-sunward speeds of $\sim$100 to 200 km/s, the MESSENGER magnetic field rotations imply spatial scale lengths of $\sim$0.2 to 2 R_M. The duration of the rotations, $\sim$5 to 25 s, is much shorter in absolute terms than is observed at Earth. However, scaled relative to the dimensions of these magnetospheres, the vortex-like signatures at Mercury imply larger scale lengths of $\sim$0.1 to 1.3 R_N than the $\sim$0.1 to 0.5 R_N found at Earth. This difference is important because at Earth the temporal and spatial scales for K-H instability are sufficiently long that MHD theory is applicable. However, the small dimensions of Mercury's magnetosphere, the large gyro-radii of planetary ions, and the low cyclotron frequencies all suggest that fully kinetic models will be required [*Fujimoto et al.*, 1998; *Glassmeier and Espley*, 2006].

[15] Near the dawn terminator a $\sim$1,000 km thick boundary layer region of reduced magnetic field intensity was encountered just prior to MESSENGER exiting the magnetosphere. The start of this BL is marked by a current sheet that resembles a rotational discontinuity. It ends with a tangential discontinuity-type current sheet consistent with expectations for an Earth-like non-reconnecting MP under northward IMF B_z. The rotational discontinuity nature of the inner current sheet with its large normal magnetic field component indicates that the BL magnetic field is connected to the inner magnetosphere. *Slavin et al.* [2008] suggested that this BL might be a "double magnetopause." In such a case, the solar wind protons would be deflected at the outer MP current sheet, while planetary ions picked up in the magnetosheath flow penetrate inward to a depth of 1 gyroradius, or about 1,000 km for Na^+ picked up in 300-km/s magnetosheath flow near the terminator, to depress the magnetic field intensity in the outer magnetosphere and form the boundary layer.

[16] The observed reduction in magnetic field strength requires an enhanced plasma pressure in the BL of $\sim$1.4 nPa to achieve pressure balance. *Slavin et al.* [2008] argued that this plasma pressure could come from the ram pressure associated with a flux of Na^+ ions incident from the magnetosheath at a density of 0.1–1 cm^{-3} and speeds of $\sim$300–400 km/s. Alternatively, hybrid simulations find significant access of solar wind plasma via gradient-curvature drift entry and cusp processes and predict densities just inside the MP that may approach that of the magnetosheath [*Trávníček et al.*, 2007]. However, *Zurbuchen et al.* [2008b] report FIPS H^+ densities and temperatures in the BL region of only $\sim$2 cm^{-3} and $\sim 5 \times 10^5$ K. The corresponding H^+ thermal pressure of 0.01 nPa is less than 1% of the 1.4 nPa required to achieve pressure balance across the inner current sheet. While this result argues against solar wind plasma entry as the cause of the boundary layer, direct measurements of the pressure contributed by planetary pickup ions will be required to understand this unexpected aspect of Mercury's magnetosphere.

[17] **Acknowledgments.** Data visualization and graphics support by C. Liebrecht and K. Feggans are gratefully acknowledged. The MESSENGER project is supported by the NASA Discovery Program under contracts NAS5-97271 to the Johns Hopkins University Applied Physics Laboratory and NASW-00002 to the Carnegie Institution of Washington.

References

Anderson, B. J., et al. (2008), The structure of Mercury's magnetic field from MESSENGER's first flyby, *Science*, *321*, 82–85.

Fujimoto, M., T. Terasawa, T. Mukai, Y. Saito, T. Yamamoto, and S. Kokubun (1998), Plasma entry from the flanks of the near-Earth magnetotail: Geotail observations, *J. Geophys. Res.*, *103*(A3), 4391–4408.

Glassmeier, K.-H., and J. Espley (2006), ULF waves in planetary magnetospheres, in *Magnetospheric ULF Waves: Synthesis and New Directions*, *Geophys. Monogr. Ser.*, vol. 169, edited by K. Takahashi et al., pp. 341–349, AGU, Washington, D. C.

Howe, H. C., and J. H. Binsack (1972), Explorer 33 and 35 plasma observations of magnetosheath flow, *J. Geophys. Res.*, *77*, 3334–3344.

Otto, A., and D. H. Fairfield (2000), Kelvin-Helmholtz instability at the magnetotail boundary: MHD simulation and comparison with Geotail observations, *J. Geophys. Res.*, *105*, 21,175–21,190.

Baker, D. N., et al. (2008), The space environment of Mercury: Solar wind and IMF modeling of upstream conditions, *Eos Trans. AGU*, *89*, Fall Meeting Suppl., Abstract U12A-01.

Russell, C. T. (1977), On the relative locations of the bow shocks of the terrestrial planets, *Geophys. Res. Lett.*, *4*, 387–390.

Sarantos, M., J. A. Slavin, M. Benna, S. A. Boardsen, and R. M. Killen (2008), Distribution of sodium pickup ions during MESSENGER's first and second Mercury flybys: Constraints on exospheric models, *Eos Trans AGU*, *89*, Fall Meeting suppl., abstract U21A-0043.

Slavin, J. A., and R. E. Holzer (1979), The effect of erosion on the solar wind stand-off distance at Mercury, *J. Geophys. Res.*, *84*, 2076–2082.

Slavin, J. A., and R. E. Holzer (1981), Solar wind flow about the terrestrial planets: 1. Modeling bow shock position and shape, *J. Geophys. Res.*, *86*, 11,401–11,418.

Slavin, J. A., R. E. Holzer, J. R. Spreiter, and S. S. Stahara (1984), Planetary mach cones: Theory and observation, *J. Geophys. Res.*, *89*, 2708–2714.

Slavin, J. A., et al. (2008), Mercury's magnetosphere after MESSENGER's first flyby, *Science*, *321*, 85–89.

Trávníček, P., P. Hellinger, and D. Schriver (2007), Structure of Mercury's magnetosphere for different pressure of the solar wind: Three dimensional hybrid simulations, *Geophys. Res. Lett.*, *34*, L05104, doi:10.1029/2006GL028518.

Zieger, B., K. C. Hansen, O. Cohen, T. I. Gombosi, and T. H. Zurbuchen (2008), Upstream solar wind conditions at Mercury during the first two MESSENGER flybys, *Eos Trans AGU*, *89*, Fall Meeting suppl., abstract U21A-0035.

Zurbuchen, T. H., et al. (2008a), MESSENGER observations of the compositions of Mercury's ionized exosphere and plasma environment, *Science*, *321*, 90–92.

Zurburchen, T. H., J. M. Raines, G. Gloeckler, S. M. Krimigis, R. L. McNutt Jr., and S. C. Solomon (2008b), Insights into the ion composition and plasma environment of planet Mecury from MESSENGER, *Eos Trans AGU*, *89*, Fall Meeting suppl., abstract U21A-08.

M. H. Acuña and M. Benna, Solar System Exploration Division, NASA Goddard Space Flight Center, Mail Code 696, Greenbelt, MD 20771, USA.

B. J. Anderson, R. E. Gold, G. C. Ho, H. Korth, S. M. Krimigis, and R. L. McNutt Jr., Johns Hopkins University Applied Physics Laboratory, Laurel, MD 20723, USA.

D. N. Baker, Laboratory for Atmospheric and Space Physics, University of Colorado, Boulder, CO 80303, USA.

S. A. Boardsen, M. Sarantos, and J. A. Slavin, Heliophysics Science Division, NASA Goddard Space Flight Center, Mail Code 670, Greenbelt, MD 20771, USA. (james.a.slavin@nasa.gov)

G. Gloeckler, J. M. Raines, and T. H. Zurbuchen, Department of Atmospheric, Oceanic and Space Sciences, University of Michigan, Ann Arbor, MI 48109, USA.

D. Schriver, Institute for Geophysics and Planetary Physics, University of California, Los Angeles, CA 90024, USA.

S. C. Solomon, Department of Terrestrial Magnetism, Carnegie Institution of Washington, 5241 Broad Branch Road, NW, Washington, DC 20015, USA.

P. Trávníček, Astronomical Institute, Academy of Sciences of the Czech Republic, CZ-141 31 Prague, Czech Republic.